Supporting Information

Effect of Local pH Change in non-PGM Catalysts – A Potential Dependent Mechanistic Analysis of the Oxygen Reduction Reaction

*J. Anjana and Azhagumuthu Muthukrishnan**

School of Chemistry, Indian Institute of Science Education and Research

Thiruvananthapuram, Vithura – 695551, Maruthamala P.O. Thiruvananthapuram, Kerala, India

Email: muthukrishnan@iisertvm.ac.in

Table of Contents

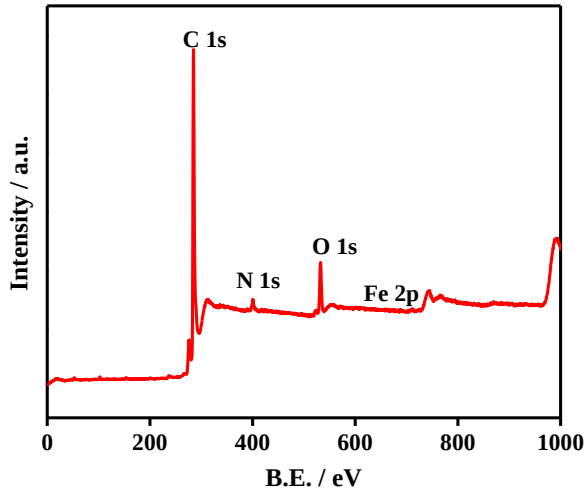

Figure S1. XPS survey spectrum of Fe/PPy-900

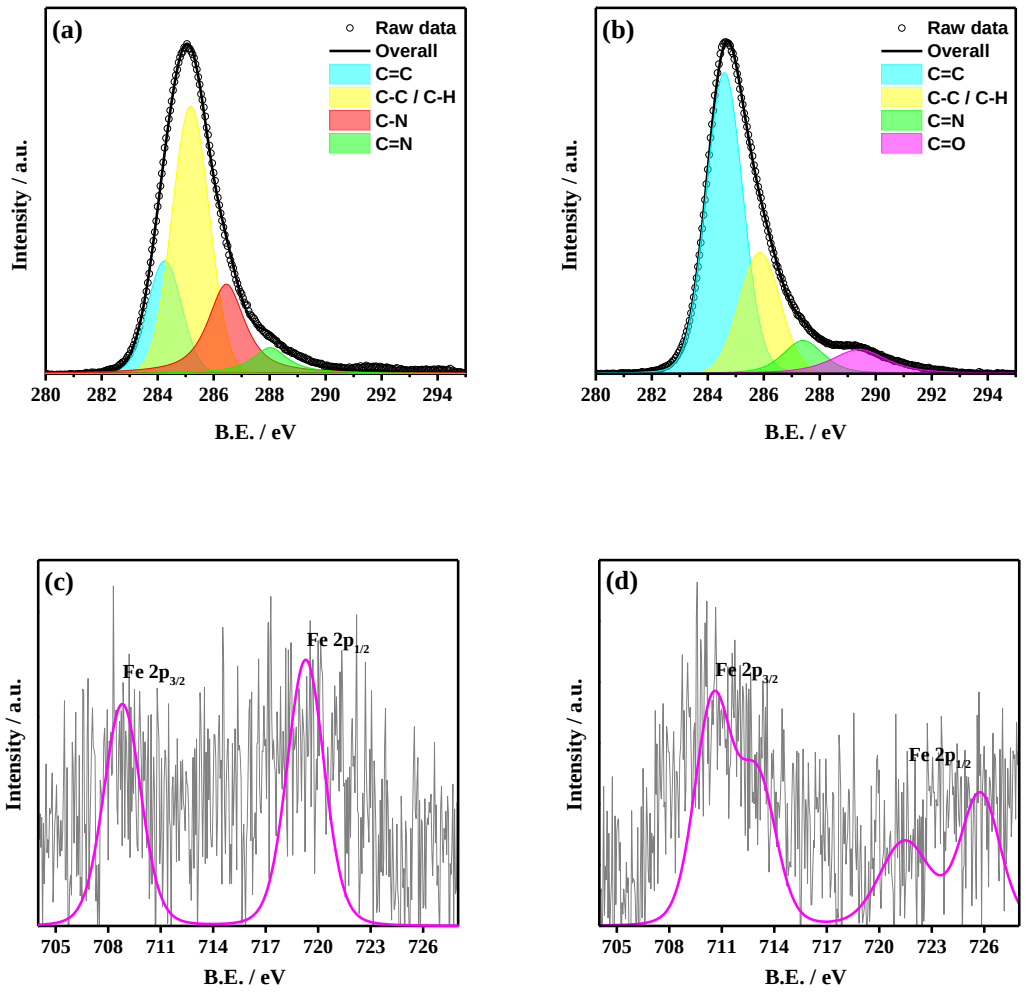

Figure S2. The core-level C 1s XPS spectra (a, b) and Fe 2p XPS spectra (c, d) of Fe/PPy (a, c) and Fe/PPy-900 (b, d)

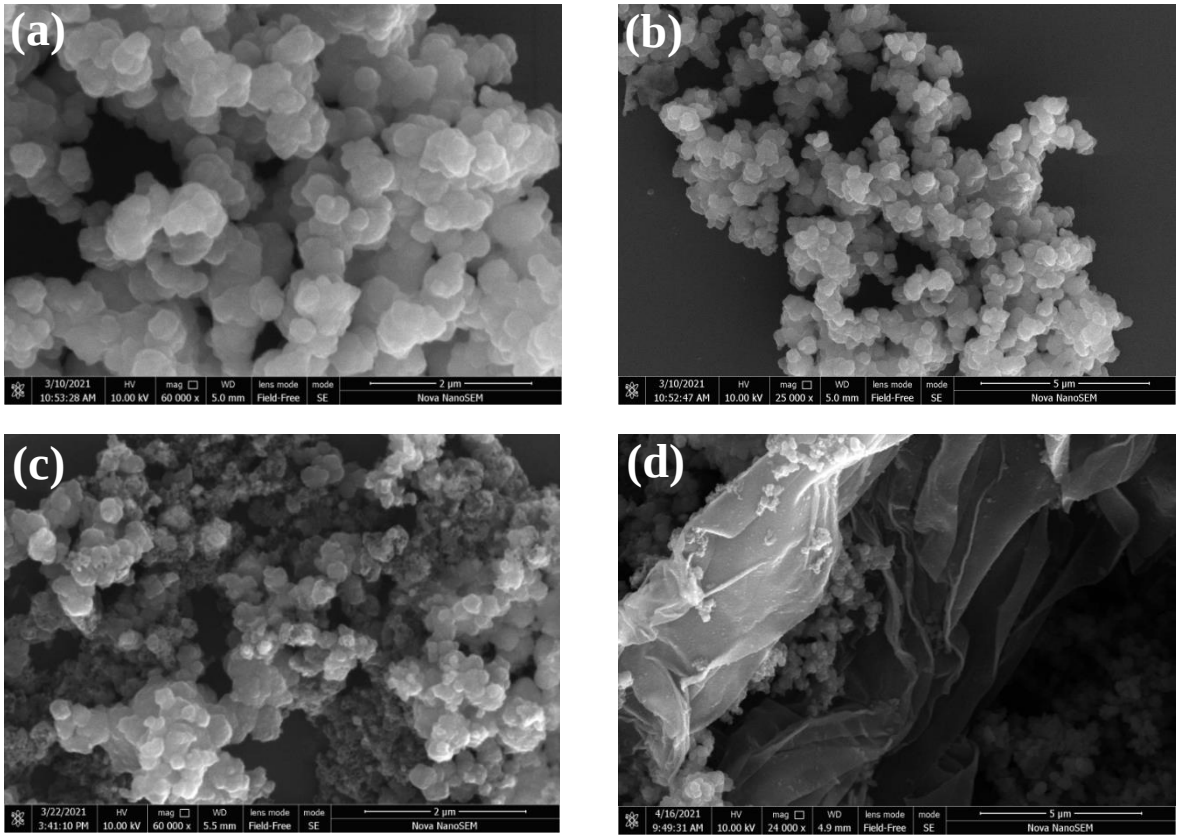

Figure S3. The Scanning electron microscopic images of Fe/PPy (a, b) and Fe/PPy-900 (c, d)

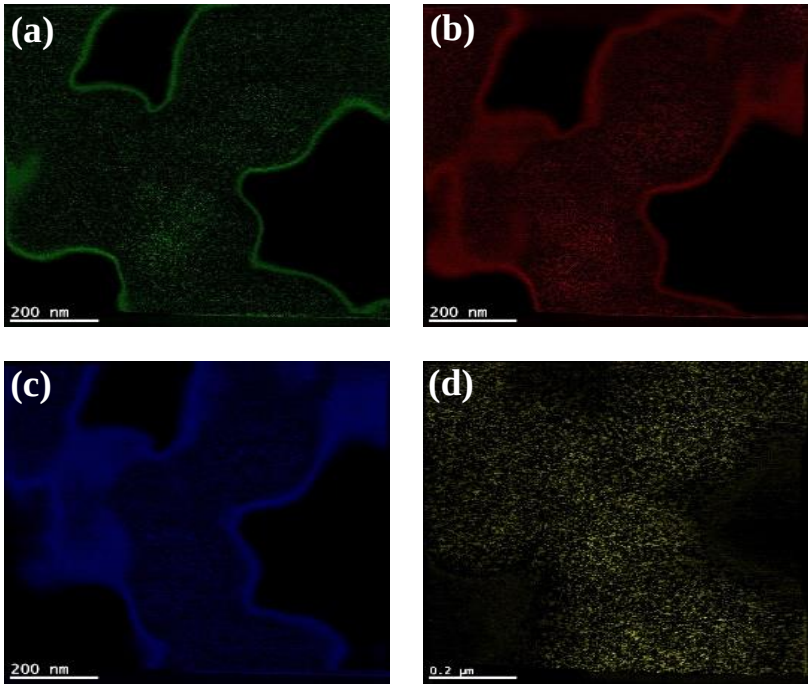

Figure S4. The EELS elemental mapping of Fe/PPy-900 for the elements (a) carbon, (b) nitrogen, (c) oxygen and (d) iron.

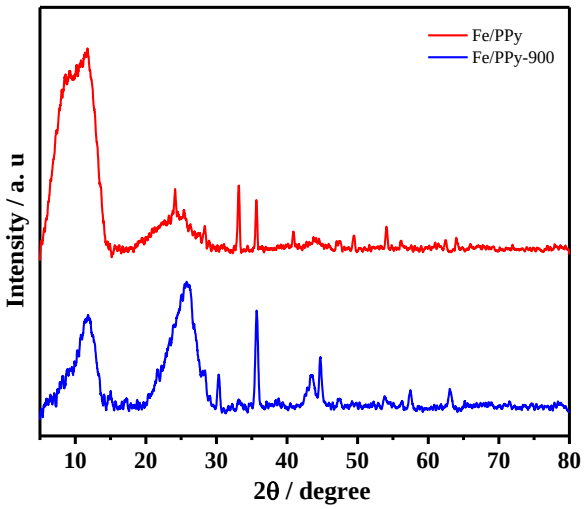

Figure S5. The powder X-ray diffraction patterns of Fe/PPy and Fe/PPy-900

The X-ray diffraction (XRD) experiments were carried out to characterize the crystalline nature of the compounds. Fe/PPy-900 shows crystalline peaks which corresponds to Fe species present in the catalyst with the typical graphitic carbon peaks at 2θ = 11.8 (001), 25.6 (002) and 43.8 (100). The high intense peak at 11.8 indicates the presence of oxygen functionalities. More crystalline peaks appear at 30.3 (corresponds to Fe_2O_3), 35.8 (Fe_3O_4), 43.2 (Fe_2O_3 or Fe nitrides), 44.7 (Fe nanoparticles or Fe nitrides), and less intense peaks at 53.9, 57.4 and 63.1 which corresponds to the Fe oxides.

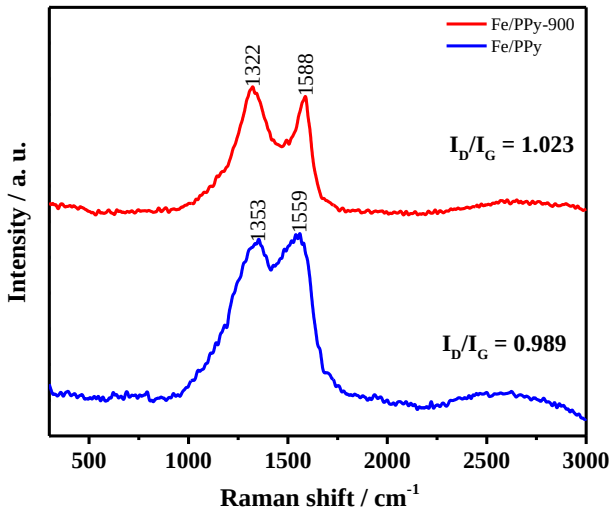

Figure S6. The Raman spectra of Fe-polypyrrole composite before (Fe/PPy) and after heat-treatment (Fe/PPy-900)

The Fe/PPy shows the characteristic peaks at 1353 and 1559 cm^{-1} corresponds to ring stretching and C=C backbone stretching mode of PPy. In the heated compound, the peaks are obtained at 1322 (D band) and 1588 cm^{-1} (G band). The I_D/I_G ratio improves from 0.98 to 1.02 after the heat treatment, which indicates that there are defects introduced in the system.

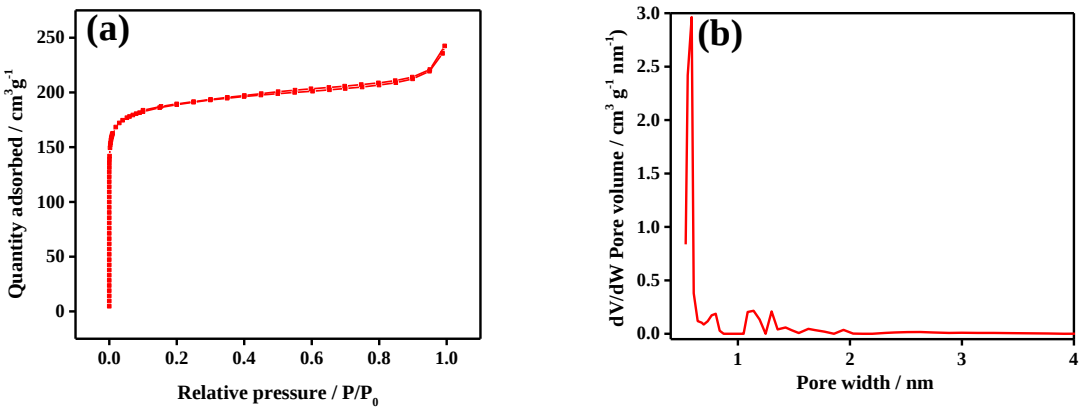

Figure S7. (a) BET adsorption isotherm and (b) NL-DFT pore size distribution of Fe/PPy-900

BET adsorption studies reveals that the Fe/PPy-900 contains almost only micropores and very less number of mesopores. Also, it has a high surface area of 672.33 m^2/g and the pore size analysis shows that it mostly contains pores of size ranging from 0.5-1.4 nm.

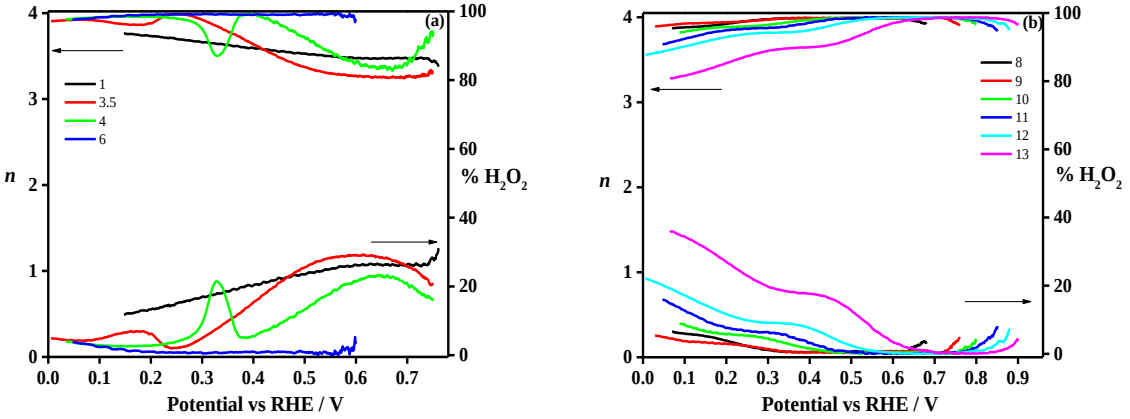

Figure S8. The number of electrons (*n*) transferred and percentage of H_2O_2 produced during ORR at (a) acidic and (b) alkaline electrolytes

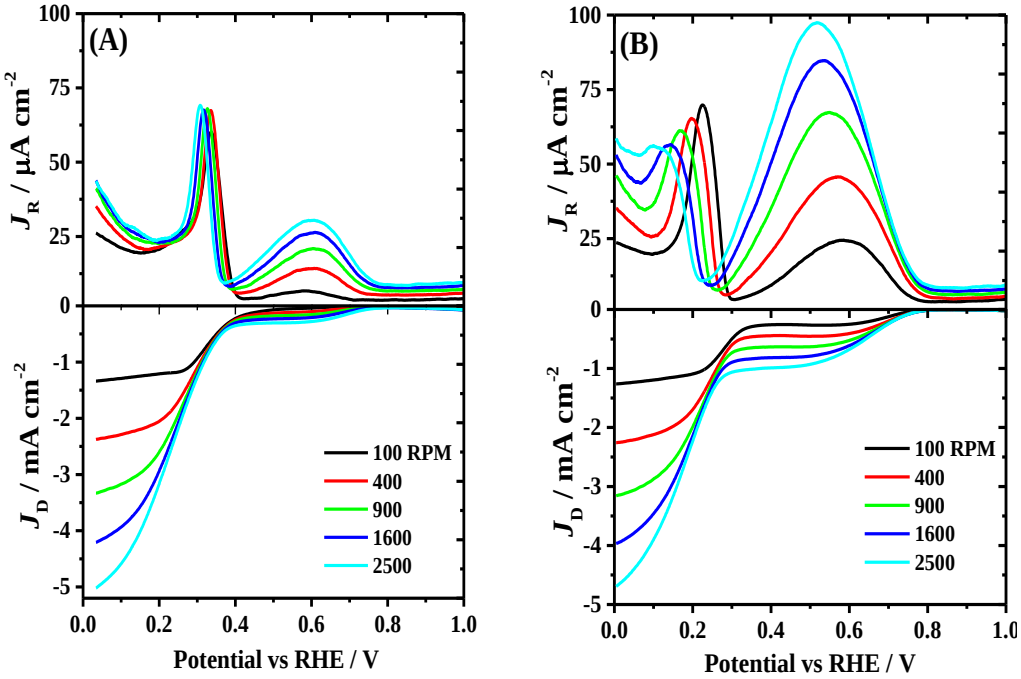

Figure S9. The RRDE voltammograms of the ORR on Fe/PPy-900 coated GC electrode in 0.1 M $KClO_4$ + $HClO_4$ (used to adjust the pH of the electrolyte) at (a) pH_b^4 and (b) $pH_b^{3.5}$. The scan rate is $0.01Vs^{-1}$.

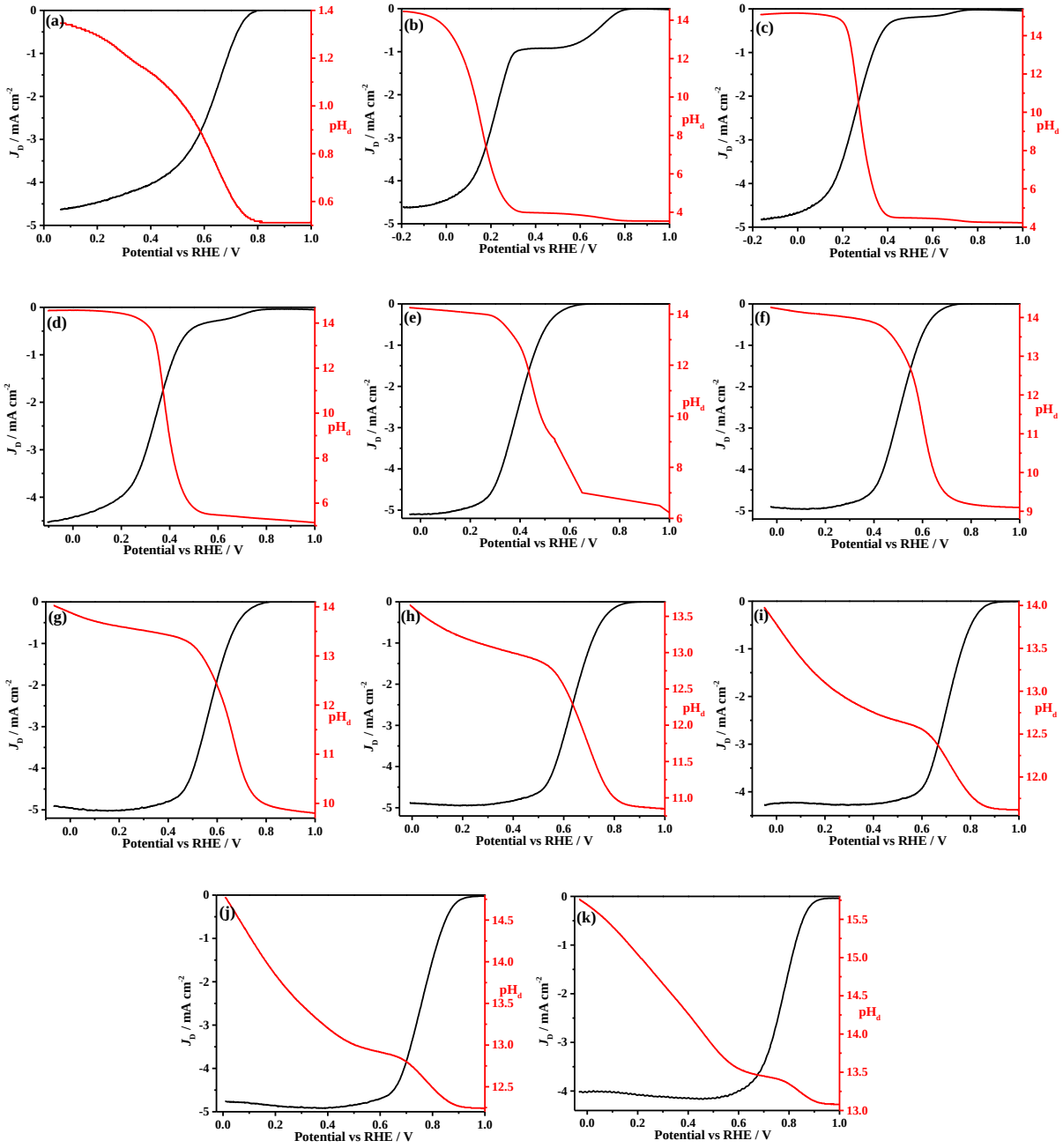

Figure S10: Local pH change with applied potential at various bulk pH electrolytes (a) pH_b^1, (b) $pH_b^{3.5}$, (c) pH_b^4, (d) pH_b^5, (e) pH_b^6, (f) pH_b^8, g) pH_b^9 (h) pH_b^{10}, (i) pH_b^{11}, (j) pH_b^{12} and (k) pH_b^{13}

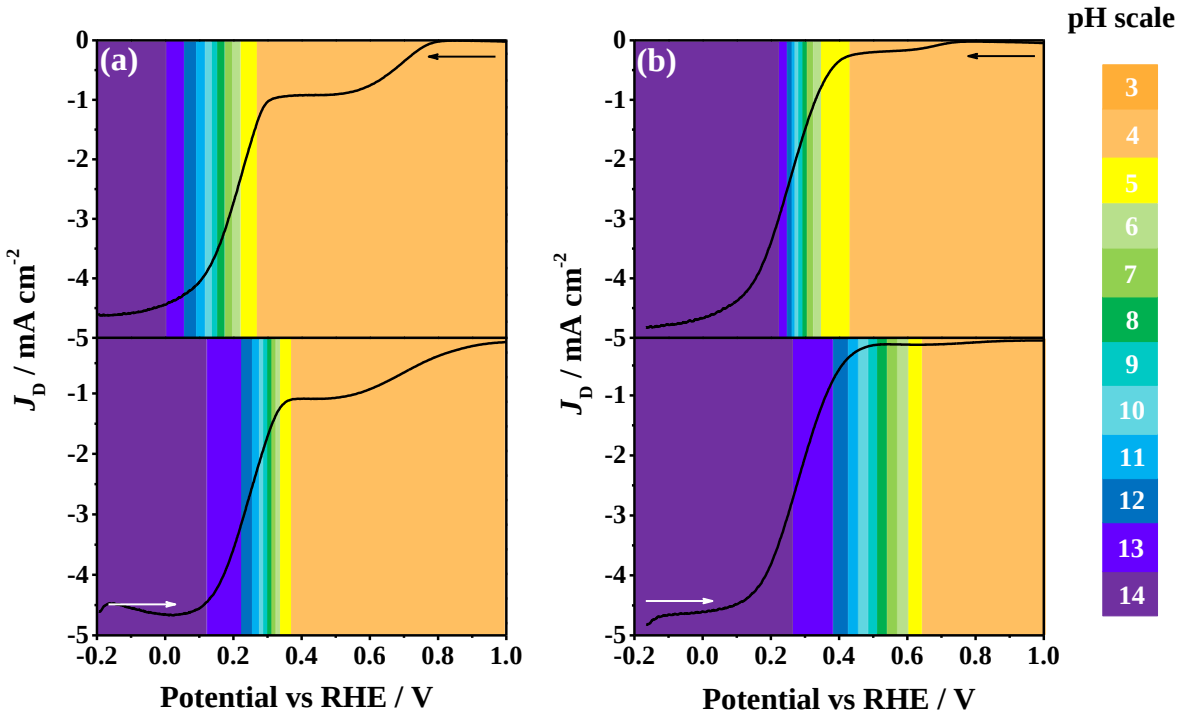

Figure S11. Mapping of the local pH change during ORR (forward and backward scans) with potential at pH (a) $\mathbf{pH_b^4}$ and (b) $\mathbf{pH_b^{3.5}}$.

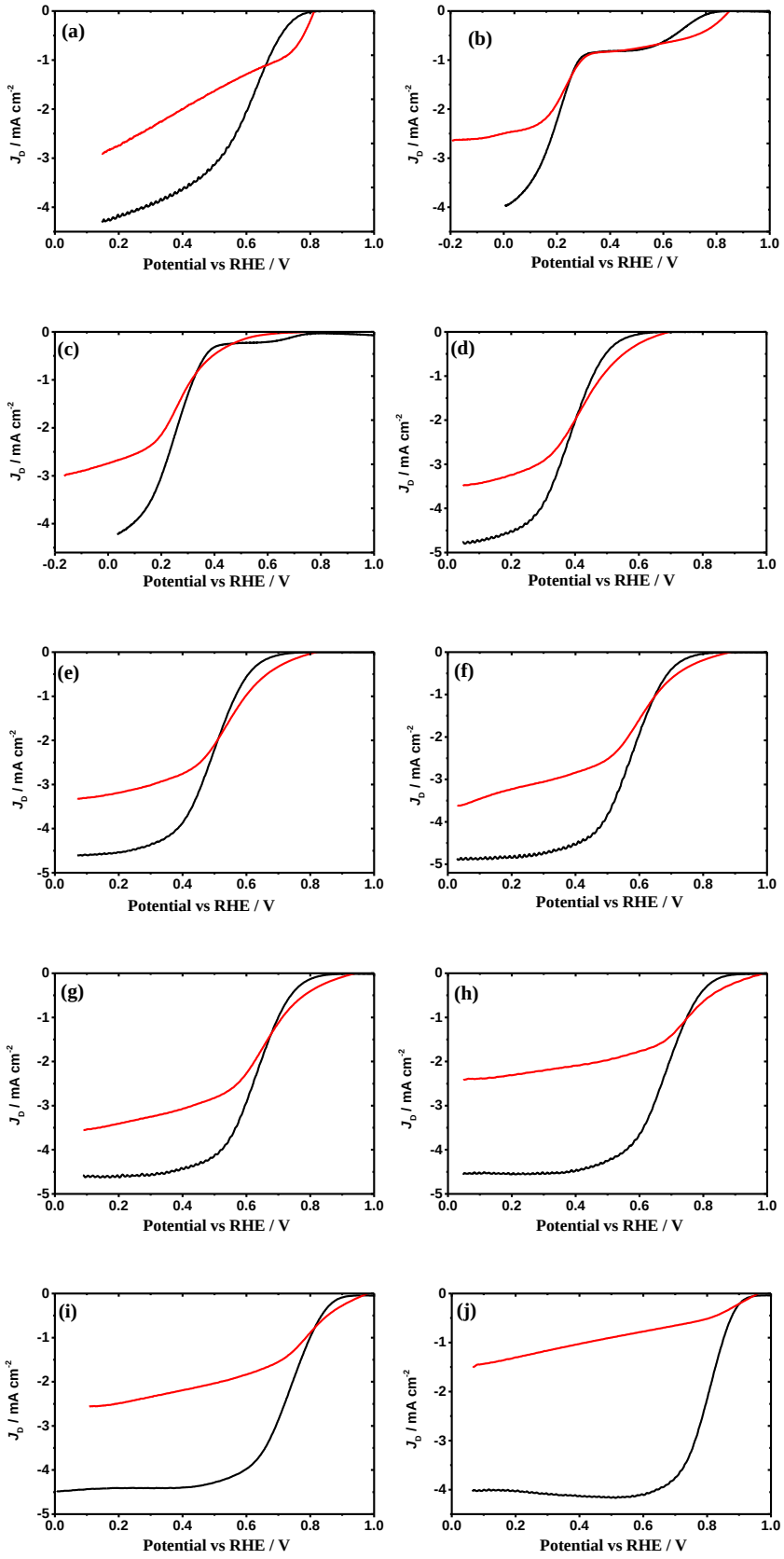

Figure S12: Comparison of RDE voltammograms of ORR (black) and H_2O_2 reduction reactions (red) with varying pH of the electrolytes (a) pH_b^1, (b) $pH_b^{3.5}$, (c) pH_b^4, (d) pH_b^6, (e) pH_b^8, (f) pH_b^9, (g) pH_b^{10}, (h) pH_b^{11}, (i) pH_b^{12} and (j) pH_b^{13}

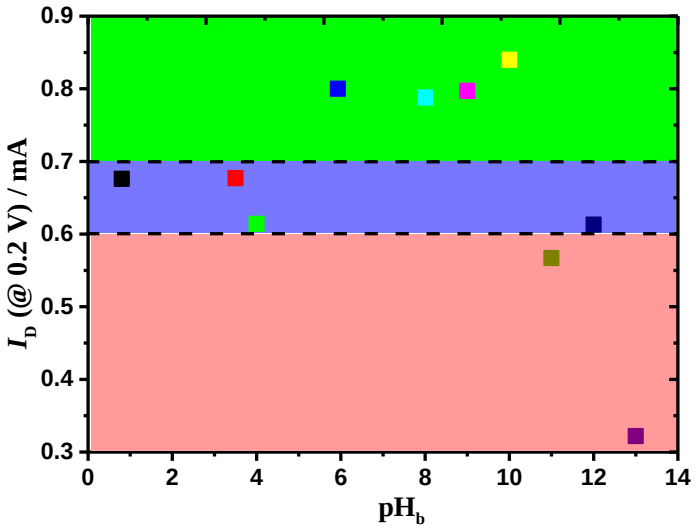

Figure S13. The current density of H_2O_2 reduction reaction at 0.2 V vs RHE (except the pH 3.5 and 4 electrolytes, taken at 0 V vs RHE).

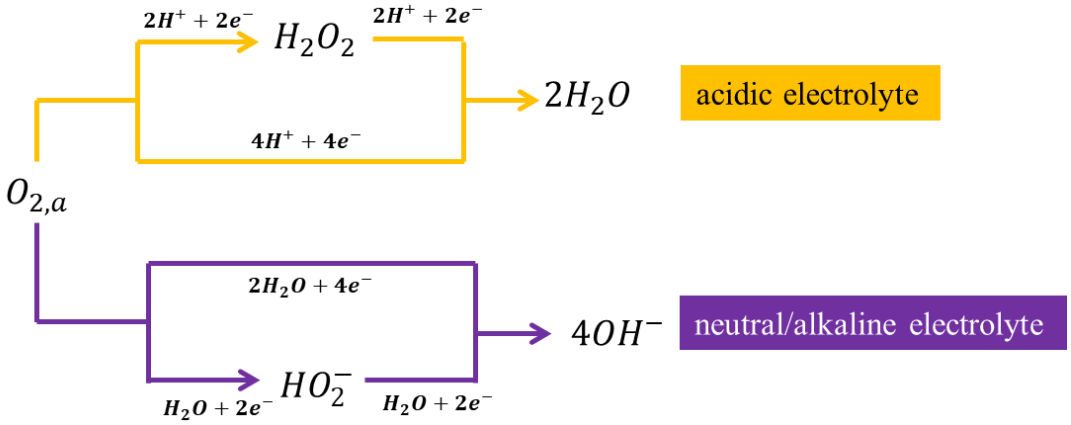

Scheme S1. The scheme for the ORR mechanism acidic and neutral/alkaline electrolytes

Estimation of number of electrons

Number of electrons (n) and percentage H_2O_2 produced are calculated by the equations

$$n = \frac{4I_D}{I_D + I_R/N}$$

$$\%\ H_2O_2 = 100\frac{2I_R/N}{I_D + I_R/N}$$

Where I_D is the faradaic current at the disk, I_R is the faradaic current at the ring and N is the collection efficiency at the ring, taken as 0.3

Estimation of local pH on the disk electrode

The calibration plot demonstrates the linear relationships of OCP_r with pH in the acidic and alkaline regions. From this relation, one can estimate the local pH of the ring electrode.

$$OCP_r = m\ pH_r + C$$

Where m and C represents the slope and intercept

$$pH_r = \frac{OCP_r - C}{m} \qquad (S1)$$

Since the OH^- ions are generated due to the ORR at neutral medium which is responsible for the local pH change, the OH^- ion concentration is taken in to account. Subsequently, the pOH will be used in this calculations,

$$pOH_r = -\log[OH^-]_r$$

Since the $[OH^-]_d = \frac{[OH^-]_r}{N}$

$$pOH_r = -\log(N[OH^-]_d)$$

$$pOH_r = -\log(0.37) - \log[OH^-]_d$$

$$pOH_r = pOH_d - \log(0.37)$$

converting into the pH scale,

$$14 - pOH_r = 14 - [pOH_d - \log(0.37)]$$

$$pH_r = pH_d + \log(0.37)$$

Hence the local pH on the disk electrode can be calculated from the local pH of the ring electrode using the following relation. The pH_r is calculated from the OCP as shown in the equation (1).

$$pH_d = pH_r + 0.432 \qquad (S2)$$

Table S1. Atomic percentage of the elements obtained from XPS data

	% C	%N	%O	%Fe
Fe/PPy	83.03	11.23	5.24	<1
Fe/PPy-900	92.13	1.88	5.23	<1

Table S2. Percentage of different types of nitrogen obtained from XPS data

	Py-N	Im-N	-N-H+	Pr-N	Gr-N	Fe-N	N-O
Fe/PPy	-	1.76	9.37	88.87	-	-	-
Fe/PPy-900	14.85	-	-	-	56.63	12.95	15.57

Py-N – Pyridinic, Im – imine, Pr – pyrrolic, Gr – graphitic, N-O – nitrogen oxides

Table S3. The RRDE voltammograms onset potentials of the ORR at different electrolytic pH values.

pH of electrolyte	$E_{onset}^{O_2}$
1	0.80
3.5	0.79
4	0.76
6	0.66
8	0.75
9	0.79
10	0.84
11	0.91
12	0.94
13	0.98

Table S4. Tafel slopes calculated from the plot shown in Figure 6.

pH of the electrolyte	Tafel slope mV dec^{-1}
1	-57
3.5	-69
4	-151
6	-94
8	-96
9	-92
10	-92
11	-88
12	-85
13	-69